Chemical Engineering Science 101 (2013) 851–864

Contents lists available at ScienceDirect

Chemical Engineering Science

journal homepage: www.elsevier.com/locate/ces

# Solubility of carbon dioxide in aqueous blends of 2-amino-2-methyl-1-propanol and piperazine

Danlu Tong [a,b], Geoffrey C. Maitland [a], Martin J.P. Trusler [a,c], Paul S. Fennell [a,b,c,*]

[a] Department of Chemical Engineering, Imperial College London, Exhibition Road, London, SW7 2AZ, United Kingdom
[b] Grantham Institute for Climate Change, Imperial College London, Exhibition Road, London, SW7 2AZ, United Kingdom
[c] Imperial College Centre for Carbon Capture and Storage, Imperial College London, Exhibition Road, London, SW7 2AZ, United Kingdom

## HIGHLIGHTS

- New solubility data for carbon dioxide in aqueous blends of AMP and PZ are reported.
- The replacement of AMP with PZ reduced the $CO_2$ mole-ratio loading capacity.
- The mole-ratio loading of the (AMP +PZ) blend still compares favourably with MEA.
- The experimental data are correlated with Kent–Eisenberg model.

## GRAPHICAL ABSTRACT

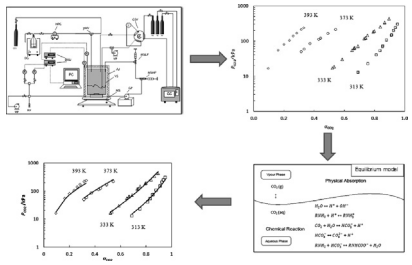

## ARTICLE INFO

*Article history:*
Received 18 March 2013
Received in revised form
14 May 2013
Accepted 17 May 2013
Available online 5 June 2013

*Keywords:*
Gas absorption
Vapour–liquid equilibria
Sterically-hindered amines
AMP
PZ
Kent–Eisenberg model

## ABSTRACT

In this work, we report new solubility data for carbon dioxide in aqueous blends of 2-amino-2-methyl-1-propanol (AMP) and piperazine (PZ). A static-analytical apparatus, validated in previous work, was employed to obtain the results at temperatures of (313.2, 333.2, 373.2, 393.2) K, and at total pressures up to 460 kPa. Two different solvent blends were studied, both having a total amine mass fraction of 30%: (25 mass% AMP+5 mass% PZ) and (20 mass% AMP+10 mass% PZ). Comparisons between these PZ activated aqueous AMP systems and 30 mass% aqueous AMP have been made in terms of their cyclic capacities under typical scrubbing conditions of 313 K in the absorber and 393 K in the stripper. The Kent–Eisenberg model was used to correlate the experimental data.



## 1. Introduction

Sterically-hindered amines are considered as a promising category of amines (Sartori and Savage, 1983) for $CO_2$ capture, and potentially possess as much as twice the theoretical cyclic capacity of monoethanolamine (MEA) on a molar basis. AMP is the most well-known of these sterically-hindered amines in the context of $CO_2$ capture processes, owing to the fact that it is the simplest hindered form of MEA,

* Corresponding author at: Department of Chemical Engineering, Imperial College London, Exhibition Road, London, SW7 2AZ, United Kingdom. Tel.: +44 20 7594 6637; fax: +44 20 7594 5638.
*E-mail address:* p.fennell@imperial.ac.uk (P.S. Fennell).

0009-2509 
http://dx.doi.org/10.1016/j.ces.2013.05.034

and the difference in properties can be attributed to the steric hindrance. As a primary amine, it is generally agreed that the direct reaction between AMP and $CO_2$ to form carbamate is possible. This was verified by Xu et al. (1996) who studied the absorption of $CO_2$ in the nonaqueous solvent blend (AMP+1-propanol). Not only were the reaction kinetics well represented with the zwitterions mechanism, but also white carbamate precipitate was observed during their experiment. In the previous studies, two mechanisms have been proposed for the AMP-carbamate formation reaction.

The first mechanism, AMP-I, is the zwitterion reaction originally proposed by Caplow (1968). He assumed that a hydrogen bond is formed between the amine and a water molecule prior to its reaction with $CO_2$:

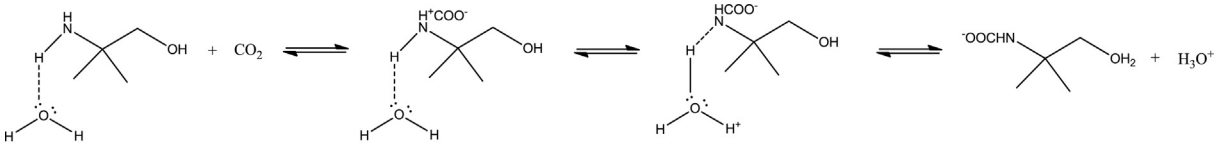


(I)

In the above scheme, the proton transfer within a hydrogen-bonded complex is exceedingly rapid in the equilibrium-favoured direction; whereas the first step is rate-limiting, and involves nucleophilic attack on the carbon atom by the nitrogen atom which leads to the formation of the zwitterion. Later studies (Sartori and Savage, 1983; Littel et al., 1992) assumed that the zwitterion formation reaction takes place without hydrogen bonding between the amine and water. This is then followed by deprotonation of the zwitterions by a base molecule:

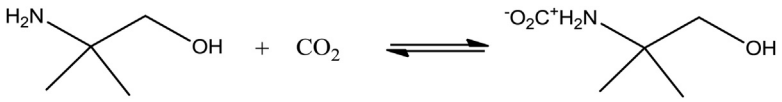


(II)

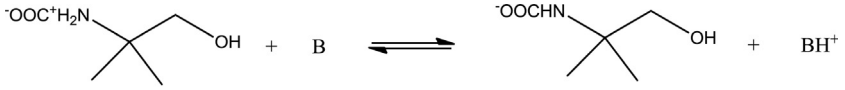


(III)

Here, B refers to a base molecule, in this case $H_2O$, AMP or $OH^-$. The rate of deprotonation is strongly dependent upon the basicity of the molecule B and hence on the pH of the solution. The steric hindrance of both the zwitterion and molecule B also have an effect.

The second mechanism, AMP-II, is a single-step reaction proposed by Crooks and Donnellan (1989):

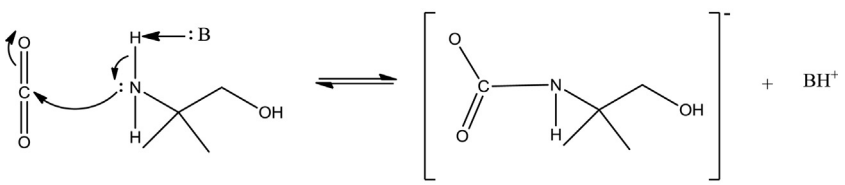


(IV)

The main difference between mechanisms I and II is that amine deprotonation takes place in a separate step as the amine reacts with $CO_2$ in the first case but these reactions happen simultaneously in the second case. Some studies suggested that the rate expression of the zwitterion mechanism fits better with the experimental data (Aboudher et al., 2003). However, it has also been argued that both mechanisms fit equally well (de Silva and Svendsen, 2004).

Although the reaction to form AMP-carbamate is viable, the extent of the reaction is much less significant than for MEA. Sharma (1961, 1964) found that steric hindrance reduced the stability of the carbamates. Chakraborty et al. (1986) reported $^{13}C$ NMR data which show that the carbamate of 2-amino-2-methyl-1-propanol is formed to a much lesser extent than the carbamate of the corresponding unsubstituted amine, i.e. monoethanolamine. Xu et al. (1992) also measured the concentration of the carbamate and found it to be only of the order of $10^{-4}$ of the amine concentration. This piece of evidence suggests that the carbamates of sterically-hindered amines may readily undergo hydrolysis, leading to the formation of bicarbonates and free amine molecules:

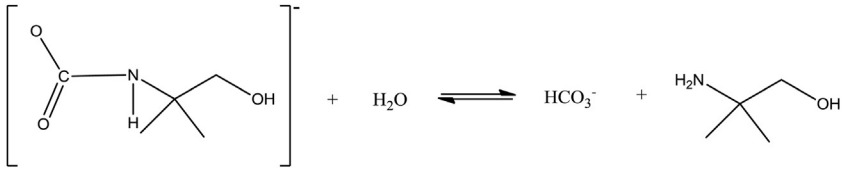


(V)

Vaidya and Kenig (2007) suggested that the zwitterion may directly undergo hydrolysis bypassing the formation of carbamate:

$$AmH^+COO^- + H_2O \rightleftharpoons HCO_3^- + AmH_2^+ \quad \text{(VI)}$$

Sartori and Savage (1983) attributed the instability of the carbamates to steric hindrance caused by the substitution on the α-carbon adjacent to the amino group. Chakraborty et al. (1986) investigated effects of substituents on the α-carbon using a molecular orbital approach. They concluded that the interaction of the lone-pair orbital with the unfilled methyl group orbitals should lead to a lower charge at the donor site. Applying hard and soft acid–base theory, they found that the effects of methyl substitution at the α-carbon atom make the amine a softer base. Since $CO_2$ falls into the hard acid category, therefore, the softer the base, the weaker the N-C bond in the zwitterion/carbamate. Moreover, $OH^-$ as a hard base reacts more favourably with $CO_2$ to form bicarbonate.

Apart from directly reacting with $CO_2$, AMP may contribute to the $CO_2$ dissolution process via increasing solution pH and the base catalytic effect, shown respectively in mechanisms III and IV.

Mechanism AMP-III describes the process of AMP protonation which leads to the rise in the solution pH and favours the formation of $H_2CO_3/HCO_3^-$:

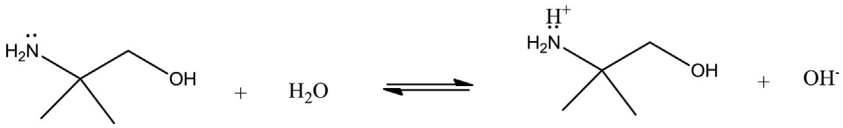


(VII)

$$CO_2 + H_2O \rightleftharpoons H_2CO_3 \quad \text{(VIII)}$$

$$CO_2 + OH^- \rightleftharpoons HCO_3^- \quad \text{(IX)}$$

Mechanism AMP-IV shows the base catalytic effect of AMP and is similar to (IV) except that the functions of $H_2O$ and AMP are reversed. This is believed to be less favourable than (IV), since AMP has stronger nucleophilicity than $H_2O$:


(X)

The $CO_2$ absorption capacity and rate in aqueous AMP has been investigated extensively in previous studies (Silkenbäumer et al., 1998; Li and Chang, 1994; Tong et al., 2012; Kundu et al., 2003; Aroonwilas and Tontiwachwuthikul, 1998; Yih and Shen, 1988; Samanta and Bandyopadhyay, 2009). Tong et al. (2012) compared the theoretical cyclic capacity of AMP with MEA and showed that the former is at least twice the latter. Despite the potential capacity, the $CO_2$ absorption rate of AMP is considerably slower than MEA leading to 'waste' of absorption capacity. Xu et al. (1996) compared three sterically-hindered amines in a concentration range of (0.25–3.5) kmol/m$^3$ at 298 K and found absorption rate constants as follows: $k_{AMP}$ (810.4 m$^3$/kmol s) < $k_{DEA}$ (2375 m$^3$/kmol s) < $k_{DIPA}$ (2585 m$^3$/kmol s). Although much higher than that of MDEA ($k_{MDEA}$ at 298 K = 18.2 m$^3$/kmol•s as measured by Mimura et al. (1998)), the reaction rate of AMP is much slower than MEA ($k_{MEA}$ at 298 K = 3630 m$^3$/kmol•s as measured by Mimura et al. (1998)).

To enhance the reaction rate of AMP, an activator is often added, normally primary (e.g. MEA) or secondary amines (e.g. DEA) with fast kinetics. Piperazine has been identified as an effective promoter by many previous investigators (Lensen, 2004; Dash et al., 2011; Cullinane and Rochelle, 2006; Bishnoi and Rochelle, 2004). It is a diamine and can react with $CO_2$ to form both single and dicarbamate products:

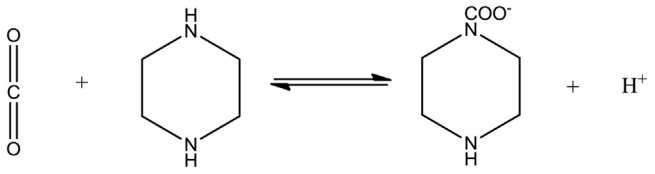


(XI)

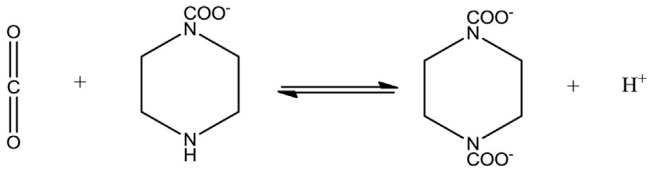


(XII)

Besides, it can protonate to form single, diprotonated PZ and protonated PZ-carbamate:

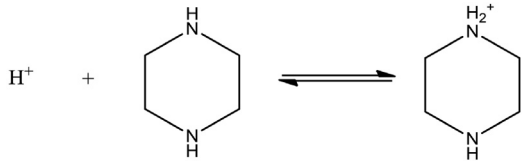


(XIII)

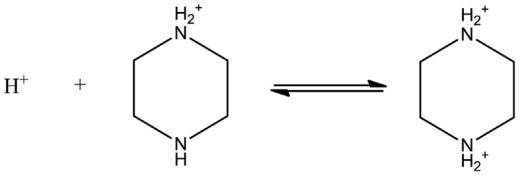

(XIV)

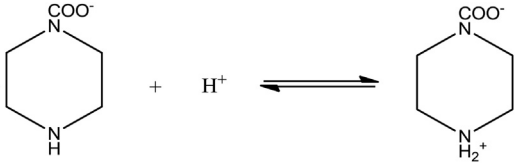

(XV)

Bishnoi and Rochelle (2000) measured the rate constant of $CO_2$ absorption in aqueous piperazine and concluded that PZ is an effective promoter because of its large rate constant (i.e. an order of magnitude higher than primary amines such as MEA or DGA®) and comparable first carbamate stability. Samanta and Bandyopadhyay (2009) measured the reaction rate of absorption of $CO_2$ into PZ activated aqueous AMP solutions using a wetting wall contactor. They found that by replacing 2 mass% AMP with 2 mass% PZ, the reaction rate increased to 3.3 times of the original for 30 mass% AMP; replacing a further 3 mass% of AMP with PZ increased the rate to 4.6 times of the original; and replacing 8 mass% of AMP with PZ increased the rate to 5.6 times the AMP reference value. In other studies, it has been observed that at comparable conditions of temperature, PZ concentration and $CO_2$ partial pressure, the (PZ+AMP) blends exhibit larger absorption flux than PZ in isolation (Samanta and Bandyopadhyay, 2009; Samanta and Bandyopadhyay, 2007; Puxty and Rowland, 2011), i.e. the rate enhancing effect of AMP and PZ blend system is mutual. For instance in the work conducted by Puxty and Rowland (2011), the rate enhancing effect of AMP on PZ was studied. They investigated the $CO_2$ mass transfer in aqueous (PZ+AMP) blends with a model taking into account chemical reactions and diffusion in a thin falling film. They claimed that by comparing the concentration profiles in the film at the same conditions with and without AMP, the reason for the rate enhancement effect of AMP on PZ becomes clear: although the two amines have similar $pK_a$ values (i.e. 9.46 for PZ and 9.29 for AMP at 313 K), the higher concentration of AMP in the solution means that it takes the priority in accepting protons, which results in more free PZ in the solution to serve the function of enhancing mass transfer.

**Table 1**
Summary of literature for $CO_2$ solubility in aqueous AMP+PZ blends.

| Author | Concentration (mass%) | $T$/K | $P_{CO2}$/kPa |
|---|---|---|---|
| Dash et al. (2011) | 38 wt% AMP+2 wt% PZ,<br>35 wt% AMP+5 wt% PZ,<br>32 wt% AMP+8 wt% PZ | 313 | 0.127–140.4 |
| Yang et al. (2010) | 22.9 wt% AMP+5.5 wt% PZ[a],<br>22.9 wt% AMP+11.1 wt% PZ[a],<br>22.9 wt% AMP+16.6 wt% PZ[a],<br>34.4 wt% AMP+5.5 wt% PZ[a],<br>34.4 wt% AMP+11.1 wt% PZ[a],<br>34.4 wt% AMP+16.6 wt% PZ[a] | 313, 333, 353 | 1.06–132.4 |

[a] Estimated from molarity based on the assumption that the density of amine solution = 1 g•ml$^{-1}$

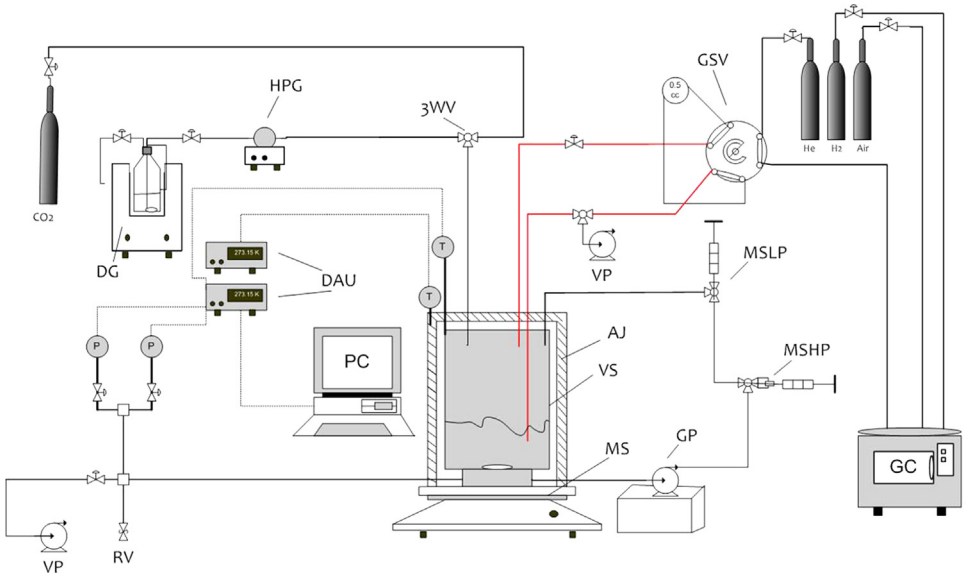


**Fig. 1.** Schematic diagram of the static-analytic apparatus. 3WV: 3-way valve; AJ: aluminium jacket; DAU: data acquisition unit; DG: degasser; GC: gas chromatograph; GP: gear pump; GSV: gas sampling valve; HPG: high pressure generator; MS: magnetic stirrer; MSHP: manual syringe for high pressure; MSLP: manual syringe for low pressure; PC: computer; VP: vacuum pump; VS: vessel.

In this work, building on our previous study of $CO_2$ in 30 mass% AMP solutions, two different (AMP+PZ) mixtures were investigated: (25 mass% AMP+5 mass% PZ) and (20 mass% AMP+10 mass% PZ). The aim was to study the influence on the theoretical $CO_2$ loading capacity at typical absorption conditions of replacing equal mass fractions of AMP with PZ. Table 1 summarises the previous solubility studies for $CO_2$ in the (AMP+PZ) system. As can be seen, most of the previous data were reported at temperatures below 373 K. In this work, both typical absorber (313–333 K) and stripper (373–393 K) temperature conditions were studied.

## 2. Experimental

### 2.1. Apparatus and procedure

The detailed experimental setup and procedures were described in our previous paper (Tong et al., 2012) and so are reviewed here only briefly. The static-analytical apparatus, shown schematically in Fig. 1, was made of stainless steel and designed for operation at temperatures from (298 to 423) K and at pressures up to 2.5 MPa. Amine solution was injected into the vessel using a manually-operated syringe pump while $CO_2$ was introduced directly from the gas-supply cylinder via a pressure-reducing regulator. An aluminium heater shell, fitted with a platinum resistance thermometer and four 100 W cartridge heaters, was used as the thermostat device and was able to regulate the temperature of the equilibrum vessel to within $\pm 0.02$ K. The cell temperature was measured with a 100 Ω platinum resistance thermometer which was calibrated by the manufacturer with a standard uncertainty of 0.05 K. Two pressure transducers, one for the range (0–0.2) MPa and the other (0–3.5) MPa, were employed to measure the pressures at low and intermediate pressures respectively. The relative standard uncertainties of the pressure were specified to be 0.03% of full range and both instruments were checked at ambient pressure before each experiment by comparison with a Delta OHM barometer having an uncertainty of 0.05 kPa. Liquid-phase samples were withdrawn through a port in the circulation line using a Pressure-Lok® precision analytical syringe. A Perkin-Elmer gas chromatograph (Clarus 500) was employed to analyse the liquid phase composition.

Approximately 90 mL of the solution was loaded into the pre-evacuated vessel at ambient temperature for each experiment. The initial pressure was below 0.1 kPa, so the remaining gas in the system was negligible. Besides, to completely remove the air in the system, the equilibrium vessel was charged with $CO_2$ and evacuated several times before finally feeding to the targeted pressure. The solution was refreshed every week to avoid errors due to degradation of the amines. The solution was brought to the desired temperature and the corresponding vapour pressure was recorded when it reached thermal equilibrium. Then $CO_2$ was introduced to the vessel from the cylinder to a desired pressure by adjusting the regulator on the gas cylinder. To ensure complete equilibration, an extended time of (10–12) h was allowed for the experiments and the final attainment of equilibrium was verified by checking stabilisation of the total pressure. For the liquid phase, at least five liquid samples were withdrawn with the manual syringe and analysed for each equilibrium point. No direct composition analysis was conducted on the gas phase; instead, since no inert gas was introduced into the system, the $CO_2$ partial pressure could be calculated by deducting the initial solvent vapour pressure from the total pressure.

As described in our previous paper (Tong et al., 2012), the relative response factor of the gas chromatograph with respect to $CO_2$ (component 1) and $H_2O$ (component 2) was determined by means of 'in-situ' calibration experiments on the $CO_2$–water binary system. This quantity is defined as

$$f_{12} = (n_1/n_2)(A_2/A_1), \tag{1}$$

where $n_i$ is the amount of component $i$ in the mixture and $A_i$ is the corresponding chromatographic peak area. The mole ratio $n_1/n_2$ in the liquid phase was determined at the calibration temperature and pressure from Henry's law using the correlation of Henry's constants reported by Carroll et al. (1991).

### 2.2. Uncertainty analysis

The combined standard uncertainty of the loading $u_c(\alpha)$ was calculated taking into account the contributions from pressure, temperature, calibration and peak-area measurements as follows:

$$u_c^2(\alpha) = \left(\frac{\partial\alpha}{\partial P}\right)^2 u^2(P) + \left(\frac{\partial\alpha}{\partial T}\right)^2 u^2(T) + \left(\frac{\partial\alpha}{\partial f_{12}}\right)^2 u^2(f_{12}) + \sum_{i=1}^{2}\left(\frac{\partial\alpha}{\partial A_i}\right) u^2(A_i). \tag{2}$$

Here, $u(P)=0.06$ kPa (for $P<200$ kPa) or 1 kPa (for $P>200$ kPa), $u(T)=0.05$ K, $u(f_{12})=0.025 f_{12}$ is the standard uncertainty of the relative response factor and $u(A_i)=0.015A_i$ is the standard uncertainty of the chromatographic peak area for component $i$. The standard uncertainty of $f_{12}$ includes both the standard deviation of peak areas during the calibration measurements and the uncertainty of the liquid-phase composition as estimated from Carroll et al. (1991). The contributions of the temperature and pressure uncertainties were estimated from the thermodynamic model (which will be discussed in Section 3) but are much smaller than the other terms. The overall standard uncertainty was found to be approximately 0.03α.

### 2.3. Experimental results

In order to evaluate the influence of replacing an amount of AMP with an equal mass concentration of PZ, two different concentrations of the amine blends were studied: 25 mass% AMP+5 mass% PZ, and 20 mass% AMP+10 mass% PZ. The measurements were made at four temperatures as summarised in Tables 2 and 3. The $CO_2$ loading, $\alpha=n_1/n_3$ was found from the measured ratio $n_1/n_2$ of $CO_2$ to $H_2O$ and the known ratio $n_2/n_3$ of $H_2O$ to total amine.

The experimental data for the (AMP+PZ) blended amine systems are plotted in Fig. 2. There appear to be no previous studies reported in the literature pertaining to the same amine concentrations as studied in this work.

**Table 2**
Solubility of $CO_2$ in aqueous (25 mass % AMP+5 mass% PZ) at $T$=(313, 333, 373 and 393) K expressed in terms of the molar loading ratio $\alpha$[a].

| $T$=313.2 K | | $T$=333.2 K | | $T$=373.2 K | | $T$=393.2 K | |
|---|---|---|---|---|---|---|---|
| $P$/kPa | $\alpha$ | $P$/kPa | $\alpha$ | $P$/kPa | $\alpha$ | $P$/kPa | $\alpha$ |
| 5.7 | 0 | 17.6 | 0 | 96.3 | 0 | 193.5 | 0 |
| 18.7 | 0.690 | 34.5 | 0.521 | 146.0 | 0.313 | 210.0 | 0.095 |
| 28.6 | 0.754 | 36.1 | 0.531 | 155.0 | 0.333 | 248.6 | 0.162 |
| 46.3 | 0.812 | 47.9 | 0.586 | 180.8 | 0.372 | 273.7 | 0.200 |
| 59.0 | 0.834 | 73.3 | 0.650 | 209.9 | 0.430 | 298.0 | 0.237 |
| 76.4 | 0.852 | 80.0 | 0.663 | 217.8 | 0.443 | 332.7 | 0.260 |
| 79.8 | 0.855 | 82.9 | 0.668 | 260.8 | 0.492 | 363.0 | 0.284 |
| 113.0 | 0.878 | 90.0 | 0.689 | 311.0 | 0.543 | 410.4 | 0.315 |
| 153.6 | 0.910 | 136.1 | 0.731 | | | 433.6 | 0.331 |
| 156.3 | 0.912 | 142.5 | 0.740 | | | | |
| 208.3 | 0.925 | 164.0 | 0.753 | | | | |
| 251.2 | 0.938 | 203.6 | 0.792 | | | | |
| 306.7 | 0.952 | 208.6 | 0.799 | | | | |
| | | 274.5 | 0.838 | | | | |
| | | 358.4 | 0.866 | | | | |

[a] Standard uncertainties are $u(T)$=0.05 K, $u(P)$=0.06 kPa (for $P<200$ kPa) or 1 kPa (for $P>200$ kPa), $u(\alpha)=0.03\alpha$.

**Table 3**
Solubility of $CO_2$ in aqueous (20 mass % AMP+10 mass% PZ) at $T$=(313, 333, 373 and 393) K expressed in terms of the molar loading ratio $\alpha$[a].

| $T$=313.2 K | | $T$=333.2 K | | $T$=373.2 K | | $T$=393.2 K | |
|---|---|---|---|---|---|---|---|
| $P$/kPa | $\alpha$ | $P$/kPa | $\alpha$ | $P$/kPa | $\alpha$ | $P$/kPa | $\alpha$ |
| 6.1 | 0 | 17.7 | 0 | 97.2 | 0 | 194.8 | 0 |
| 13.9 | 0.662 | 36.4 | 0.565 | 107.8 | 0.139 | 218.3 | 0.131 |
| 29.4 | 0.766 | 48.0 | 0.617 | 113.8 | 0.185 | 234.3 | 0.187 |
| 36.9 | 0.789 | 63.1 | 0.659 | 118.9 | 0.219 | 270.4 | 0.247 |
| 47.3 | 0.819 | 80.5 | 0.696 | 126.0 | 0.247 | 272.5 | 0.251 |
| 59.1 | 0.838 | 100.3 | 0.717 | 127.3 | 0.252 | 299.2 | 0.287 |
| 75.4 | 0.856 | 135.0 | 0.749 | 139.7 | 0.299 | 327.4 | 0.328 |
| 101.1 | 0.875 | 138.2 | 0.751 | 140.5 | 0.301 | 329.6 | 0.330 |
| 168.4 | 0.912 | 158.3 | 0.765 | 149.4 | 0.325 | 348.5 | 0.341 |
| 203.3 | 0.920 | 190.0 | 0.780 | 164.2 | 0.347 | 373.4 | 0.380 |
| 243.7 | 0.930 | 243.9 | 0.810 | 177.8 | 0.376 | 422.0 | 0.401 |
| | | 290.4 | 0.824 | 192.9 | 0.392 | | |
| | | 340.1 | 0.843 | 207.8 | 0.420 | | |
| | | 401.1 | 0.861 | 236.9 | 0.450 | | |
| | | 463.5 | 0.874 | 267.4 | 0.491 | | |
| | | | | 316.9 | 0.538 | | |
| | | | | 317.4 | 0.540 | | |

[a] Standard uncertainties are $u(T)$=0.05 K, $u(P)$=0.06 kPa (for $P<200$ kPa) or 1 kPa (for $P>200$ kPa), $u(\alpha)=0.03\alpha$.

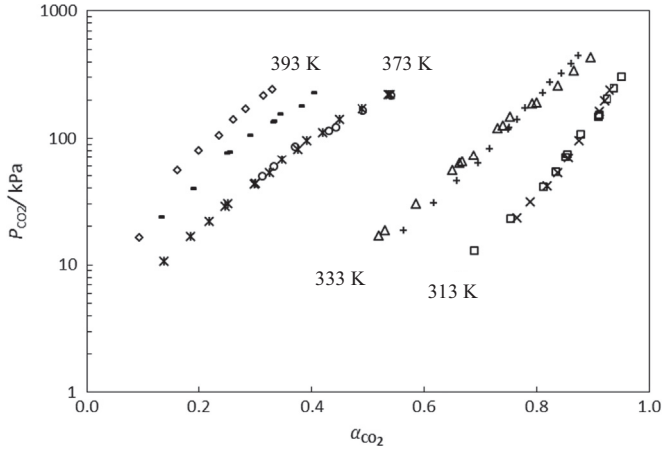


**Fig. 2.** $CO_2$ solubility in aqueous AMP and PZ blends at $T$=(313, 333, 373, and 393) K: □, △, ○, ◇ (25 mass% AMP+5 mass% PZ); ×, +, ✳, ▬ (20 mass% AMP+10 mass% PZ).

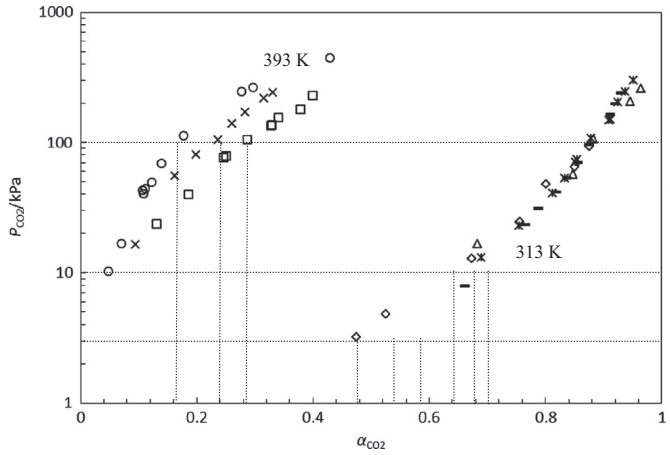


**Fig. 3.** $CO_2$ solubility in aqueous AMP and (AMP+PZ) blends at $T$=(313 and 393) K: (△, ○): this work, 30 mass% AMP; (◇): Kundu et al. (2003), 30.3 mass% AMP converted from 3.4 M AMP assuming the density of amine solution=1 g/ml; (✳, ✕): this work, 25 mass% AMP+5 mass% PZ; (▬, □): this work, 20 mass% AMP+10 mass% PZ.

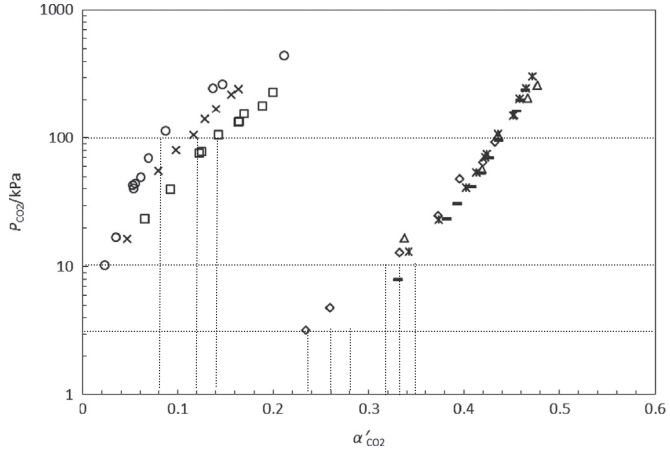


**Fig. 4.** $CO_2$ solubility in aqueous AMP and (AMP+PZ) blends at $T$=(313 and 393) K: (△, ○): this work, 30 mass% AMP; (◇): Kundu et al. (2003), 30.3 mass% AMP converted from 3.4 M AMP assuming the density of amine solution =1 g/ml; (✳, ✕): this work, 25 mass% AMP+5 mass% PZ; (▬, □): this work, 20 mass% AMP+10 mass% PZ.

**Table 4**
Comparisons of mole-ratio loadings for three aqueous AMP-based solutions.

| Loading | 30 mass% MEA[a] | 30 mass% AMP[a] | 25 mass% AMP+5 mass% PZ | 20 mass% AMP+10 mass% PZ |
|---|---|---|---|---|
| Rich loading $\alpha$(313 K, 3 kPa) | 0.52 | 0.48 | 0.53[b] | 0.58[b] |
| Rich loading $\alpha$(313 K, 10 kPa) | 0.56 | 0.64 | 0.68 | 0.7 |
| Lean loading $\alpha$(393 K, 100 kPa) | 0.36 | 0.16 | 0.24 | 0.28 |
| Cyclic capacity $\Delta\alpha$(3 kPa) | 0.16 | 0.32 | 0.29[b] | 0.30[b] |
| Cyclic capacity $\Delta\alpha$ (10 kPa) | 0.20 | 0.48 | 0.44 | 0.42 |

[a] From Tong et al. (2012).
[b] Estimated from Fig. 4.

As can be seen from Fig. 2, the solubilities of $CO_2$ in the two AMP and PZ blends having the same overall mass fraction are quite close at each temperature, except at 393 K where more PZ in the solution leads to an increase in the solution loading. A more detailed discussion of the $CO_2$ cyclic capacity for the AMP and (AMP+PZ) systems will be given in Section 2.4.

### 2.4. Comparison of cyclic capacity for aqueous AMP and (AMP+PZ) blends

To compare the theoretical $CO_2$ loading capacity of different amine systems, we define the cyclic capacity as the difference between the rich loading (at $T$=313 K and $P$=3 kPa or 10 kPa) and the lean loading (at $T$=393 K, $P$=100 kPa) expressed in terms of the mole ratio $\alpha$:

$$\Delta\alpha = \alpha(T = 313\ \text{K}, P = 3\ \text{kPaor10kPa}) - \alpha(T = 393\ \text{K}, P = 100\ \text{kPa}) \quad (3)$$

We also consider the same difference expressed in terms of the mass-ratio loading $\alpha'$:

$$\Delta\alpha' = \alpha'(T = 313\ \text{K}, P = 3\ \text{kPaor10kPa}) - \alpha'(T = 393\ \text{K}, P = 100\ \text{kPa}) \quad (4)$$

**Table 5**
Comparisons of mass-ratio loadings for three aqueous AMP-based solutions.

| Loading | 30 mass% MEA[b] | 30 mass% AMP[b] | 25 mass% AMP+5 mass% PZ | 20 mass% AMP+10 mass% PZ |
|---|---|---|---|---|
| Rich loading $\alpha'$(313 K, 3 kPa) | 0.38 | 0.24 | 0.26[a] | 0.28[a] |
| Rich loading $\alpha'$ (313 K, 10 kPa) | 0.41 | 0.32 | 0.33 | 0.35 |
| Lean loading $\alpha'$ (393 K, 100 kPa) | 0.26 | 0.08 | 0.12 | 0.14 |
| Cyclic capacity $\Delta\alpha'$ (3 kPa) | 0.12 | 0.16 | 0.14[a] | 0.14[a] |
| Cyclic capacity $\Delta\alpha'$ (10 kPa) | 0.15 | 0.24 | 0.21 | 0.21 |

[a] Estimated from Fig. 4.
[b] From Tong et al. (2012).

Fig. 3 can be used to determine the mole-ratio cyclic capacity for the three difference amine systems, while Fig. 4 can be used to determine the mass-ratio cyclic capacity. The values determined from these plots are given in Tables 4 and 5 for pressures of 3 kPa and 10 kPa.

Taking 10 kPa as an example, replacing 5 mass% of AMP with 5 mass% of PZ leads to a reduction in the cyclic capacity by about 8%, compared to that of 30 mass% AMP. A further replacement of 5 mass% reduces the capacity by another 4.5%, i.e. 12.5% smaller compared to that of 30 mass% AMP. However, according to Samanta and Bandyopadhyay(2009), the absorption rate of $CO_2$ in 20 mass% AMP+10 mass% PZ should be more than 5.6 times that in 30 mass% AMP and is equivalent to or even higher than 30 mass% MEA (estimated from $k_{AMP}=810.4\ m^3/kmol\ s$ and $k_{MEA}=3630\ m^3/kmol\ s$ both at 298 K). Despite the 'sacrifice' in the loading capacity advantage of AMP (i.e. AMP+PZ blends have smaller cyclic capacity than AMP solution at the same mass concentration), the AMP+PZ blends still benefits from larger loading capacity than MEA solutions of the same total amine mass fraction: 1.2 times and 1.1 times larger in mole-ratio cyclic capacity respectively for 25 mass% AMP+5 mass% PZ and 20 mass% AMP+10 mass% PZ compared to 30 mass% MEA.

The results in Table 5 show us that if the mass-ratio loading was used instead of the mole-ratio loading to compare the cyclic capacity of these three amine systems, the PZ activated AMP systems both have $CO_2$ absorption capacities about 12.5% smaller than the aqueous AMP solution without PZ. There is no distinguishable difference between the two (AMP+PZ) blends.

## 3. Correlation of experimental data with the Kent–Eisenberg model

### 3.1. Development of the Kent–Eisenberg model

Kent and Eisenberg (1976) built upon the work of Dankwerts and McNeil (1967) and developed a simple correlation method which accounts for all the liquid-phase non-ideality by means of certain selected equilibrium constants. Although not a predictive model in its nature, it is still frequently used in both the academic and industrial environments. In the Kent–Eisenberg model, the vapour pressures of the molecular species are proportional to the free component concentrations in the liquid phase governed by Raoult's law. The activity coefficients of all components are set to unity. Selected equilibrium constants, in most cases amine protonation constants and carbamate formation constants, were adjusted to accommodate the phase non-ideality. This greatly simplified the model as only two parameters were required for each amine. Although only mixed $CO_2$ and $H_2S$ gases in MEA or DEA solutions were discussed in the original paper, this model can be easily extended to other amines and amine mixtures.

The original Kent–Eisenberg model assumed that the equilibrium constants for reactions involving the amines were only dependent on temperature. Haji-Sulaiman et al. (1998) modified the model to incorporate the dependency on the free gas concentration in solution and the amine concentration in the expressions of equilibrium constants of amine protonation and carbamate formation. In addition, they extended the model to applications where no carbamate was formed (e.g. MDEA) as well as mixed-amine solutions (e.g. DEA–MDEA). Jou et al. (1982) further assumed the equilibrium constants to be dependent upon the $CO_2$ loading and the amine concentration, in addition to the temperature. Hu and Chakma (1990) introduced a modified expression for the equilibrium constants for the amine reactions as functions of temperature, acid-gas partial pressure and amine concentration. Li and Shen (1993) correlated $CO_2$ solubility in (MEA+MDEA) mixtures using a modified version of the Kent–Eisenberg model assuming the amine related equilibrium constants as functions of temperature, amine concentration and $CO_2$ loading. This method has been employed by Yang et al. (2010) to correlate the $CO_2$ solubility in aqueous AMP and PZ solutions.

### 3.2. Model framework

#### 3.2.1. Physical and chemical equilibria

The absorption of $CO_2$ into an amine solution includes both phase and chemical equilibria. The gas phase $CO_2$ first dissolves into the aqueous phase:

$$CO_2(g) \overset{H_{CO_2}}{\leftrightarrow} CO_2(aq) \tag{a}$$

The dissolved $CO_2$ undergoes a series of chemical reactions and forms various ionic species. For (AMP+PZ) blends, the following reactions are considered although the possible reactions are not just limited to these:

Ionisation of water:

$$2H_2O \overset{K_1}{\leftrightarrow} H_3O^+ + OH^- \tag{b}$$

Formation of bicarbonate:

$$CO_2 + 2H_2O \overset{K_2}{\leftrightarrow} H_3O^+ + HCO_3^- \quad (c)$$

Formation of bicarbonate

$$HCO_3^- + H_2O \overset{K_3}{\leftrightarrow} H_3O^+ + CO_3^{2-} \quad (d)$$

Reversion of the protonation of AMP:

$$RNH_3^+ + H_2O \overset{K_4}{\leftrightarrow} RNH_2 + H_3O^+ \quad (e)$$

Reversion of the protonation of PZ:

$$PZH^+ + H_2O \overset{K_5}{\leftrightarrow} PZ + H_3O^+ \quad (f)$$

Deformation of first order PZ-carbamate:

$$PZCOO^- + H_2O \overset{K_6}{\leftrightarrow} PZ + HCO_3^- \quad (g)$$

Deformation of second order PZ-carbamate:

$$PZ(COO^-)_2 + H_2O \overset{K_7}{\leftrightarrow} PZCOO^- + HCO_3^- \quad (h)$$

Reversion of protonation of the first order PZ-carbamate:

$$PZH^+COO^- + H_2O \overset{K_8}{\leftrightarrow} PZCOO^- + H_3O^+ \quad (i)$$

The equilibrium constants ($K_1$–$K_s$) for the above chemical reactions are defined as:

$$K_1 = m(OH^-)m(H_3O^+)/(m^0)^2 \quad (5)$$

$$K_2 = \frac{m(HCO_3^-)m(H_3O^+)}{m(CO_2)m^0} \quad (6)$$

$$K_3 = \frac{m(CO_3^{2-})m(H_3O^+)}{m(HCO_3^-)m^0} \quad (7)$$

$$K_4 = \frac{m(A)m(H_3O^+)}{m(AH^+)m^0} \quad (8)$$

$$K_5 = \frac{m(PZ)m(H_3O^+)}{m(PZH^+)m^0} \quad (9)$$

$$K_6 = \frac{m(PZ)m(HCO_3^-)}{m(PZCOO^-)m^0} \quad (10)$$

$$K_7 = \frac{m(PZCOO^-)m(HCO_3^-)}{m(PZ(COO^-)_2)m^0} \quad (11)$$

$$K_8 = \frac{m(PZCOO^-)m(H_3O^+)}{m(PZH^+COO^-)m^0} \quad (12)$$

The formation of AMP-carbamate was not taken into account here because, although its presence in the solution was identified (Xu et al., 1996), the concentration is extremely small (Xu et al., 1996; Chakraborty et al., 1986). In the mixture with PZ, competing reactions would be likely to further reduce the concentration of AMP-carbamate. Therefore, it is considered reasonable to ignore this reaction. The equilibrium constants $K_i$ ($i$=1–8) and Henry's constant $H_{CO2}$ are temperature dependent and represented in this work by the following

**Table 6**
Henry's constant and equilibrium constant parameters used in the Kent–Eisenberg model for reactions (a)–(i).

| Parameter | $a_i$ | $b_i$ | $c_i$ | $d_i$ | Range of validity (K) | Source |
|---|---|---|---|---|---|---|
| $K_1$ | −13445.9 | −22.4773 | 0 | 140.932 | 273–498 | Edwards et al. (1978) |
| $K_2$ | −12092.1 | −36.7816 | 0 | 235.482 | 273–498 | Edwards et al. (1978) |
| $K_3$ | −12431.7 | −35.4819 | 0 | 220.067 | 273–498 | Edwards et al. (1978) |
| $K_4$ | −2546.2 | 0 | 0 | 11.555 | 298–313 | Silkenbäumer et al. (1998) |
| $K_5$ | 3814.4 | 0 | −1.5016 | 14.119 | 273–323 | Kamps et al. (2003) |
| $K_6$ | 3616 | 0 | 0 | −8.635 | 283–333 | Ermatchkov et al. (2002) |
| $K_7$ | 1322.1 | 0 | 0 | −3.654 | 283–333 | Ermatchkov et al. (2002) |
| $K_8$ | −6066.9 | −2.29 | 0.0036 | 6.822 | 273–343 | Cullinane and Rochelle (2005) |
| $H_{CO2}$/(MPa kg mol$^{-1}$) | −9624.4 | −28.749 | 0.01441 | 192.876 | 273–473 | Rumpf and Maurer (1993) |

**Table 7**
Adjustable parameters in Eq. (15) for the AMP–PZ–$H_2O$–$CO_2$ system.

| Regressed adjustable parameters | $K_7'$ | $K_8'$ | $K_{13}'$ |
|---|---|---|---|
| $a_1$ | 0.3293 | 20.30 | −0.3386 |
| $a_2$ | 0 | 0 | 504.5 |
| $a_3$ | 0.02139 | −0.07474 | −0.002334 |
| $b_1$ | 0 | 0 | 0.05995 |
| $b_2$ | −0.005099 | 0.0007053 | −0.001382 |
| $c_1$ | 0 | 0 | −0.3419 |
| $c_2$ | −0.8711 | −0.01358 | −0.1997 |

empirical expression:

$$\ln K_i(\text{or} H_{CO_2}/(\text{MPa kg mol}^{-1})) = a_i(\text{K}/T) + b_i\ln(T/\text{K}) + c_i(T/\text{K}) + d_i \tag{13}$$

where $a_i$–$d_i$ are constants. Values of these constants taken from the literature are given in Table 6.

### 3.2.2. Phase non-ideality

The treatment of phase non-idealities in the Kent–Eisenberg model was significantly simplified compared to the traditional $\gamma$–$\varphi$ approach, i.e. the vapour phase non-ideality was neglected while all the non-ideality in the liquid phase was lumped into a number of selected equilibrium constants.

In this work, we chose $K_7$, $K_8$ and $K_{13}$ as adjustable equilibrium constants based on the criteria of relative importance. Considering that PZ readily reacts with $CO_2$ to form carbamate, whereas it has a smaller $pK_a$ than AMP in the blended system, reactions VII (formation of first order carbamate) and VIII (formation of second order carbamate) were selected for PZ. For AMP, as the carbamate formation was neglected, the protonation of these two amines was used to represent the non-ideality.

The original form of the Kent–Eisenberg model assumed that the adjustable equilibrium constants were merely functions of temperature. Jou et al. (1982) revised the model by introducing dependency on loading and amine concentration; however, the exact form was not described in their paper. In the work of Hu and Chakma (1990), the equilibrium constants were considered to be dependent on temperature, acid gas partial pressure and amine concentration. Li and Shen (1993) modified the Kent–Eisenberg model to be dependent on temperature, amine concentration and $CO_2$ loading. The final form of the equilibrium constants was as follows:

$$K = \exp(a_1 + a_2\text{K}/T + a_3\text{K}^3/T^3 + b_1\alpha_{CO_2} + b_2/\alpha_{CO_2} + b_3/\alpha_{CO_2}^2 + b_4\ln m/m^0) \tag{14}$$

where $a_i$, $b_i$ are adjustable parameters regressed from experimental data. In this work, we assumed the equilibrium constants are a function of temperature, $CO_2$ partial pressure and amine concentration. The adjustable equilibrium constants, $K_{i,t}$, are related to the literature values ($K_i$, calculated from Eq. (12) and parameters in Table 6) with 'deviation parameters' ($K_i'$):

$$K_{i,t} = K_iK_i' \tag{15}$$

$$K_i' = \exp(a_1 + a_2\text{K}/T + a_3\text{K}/T + b_1\ln(P_{CO_2}/\text{kPa}) + b_2(P_{CO_2}/\text{kPa}) + c_1m(\text{AMP or DMMEA})/m^0 + c_2m(\text{PZ})/m^0 \tag{16}$$

$a_i$, $b_i$ and $c_i$ are adjustable parameters obtained from regression of experimental data for both ternary (AMP–$H_2O$–$CO_2$ or DMMEA–$H_2O$–$CO_2$) and quaternary systems (AMP–PZ–$H_2O$–$CO_2$ or DMMEA–PZ–$H_2O$–$CO_2$) simultaneously. The objective function to be minimised for the Kent–Eisenberg model is based on the difference between the experimentally obtained partial pressures of $CO_2$ and that calculated from the model.

$$F = (1/N)\sum_{i=1}^{N}((P_{i,\text{exp}} - P_{i,\text{cal}})/\sigma_i)^2 \tag{17}$$

where $N$ is the total number of measurements taken during all the experiments, $P_{i,\text{exp}}$ is the experimental partial pressure, $P_{i,\text{cal}}$ is the partial pressure calculated from the model and $\sigma_i^2$ is the variance of the $i$th experimental system pressure.

### 3.2.3. Balance equations

The mass and charge balance equations also need to be observed and are expressed as follows:

Amine balance:

$$m(\text{RNH}_2) + m(\text{RNH}_3^+) + m(\text{RNHCOO}^-) = m^0(\text{RNH}_2)\ \text{(AMP)} \tag{18}$$

Carbon balance:

$$m(\text{CO}_2) + m(\text{HCO}_3^-) + m(\text{CO}_3^{2-}) + m(\text{RNHCOO}^-) = \alpha_{CO_2}m^0(\text{RNH}_2)\ \text{(AMP)} \tag{19}$$

Charge balance:

$$m(\text{RNH}_3^+) + m(\text{H}_3\text{O}^+) = m(\text{OH}^-) + m(\text{HCO}_3^-) + 2m(\text{CO}_3^{2-}) + m(\text{RNHCOO}^-)\ \text{(AMP)} \tag{20}$$

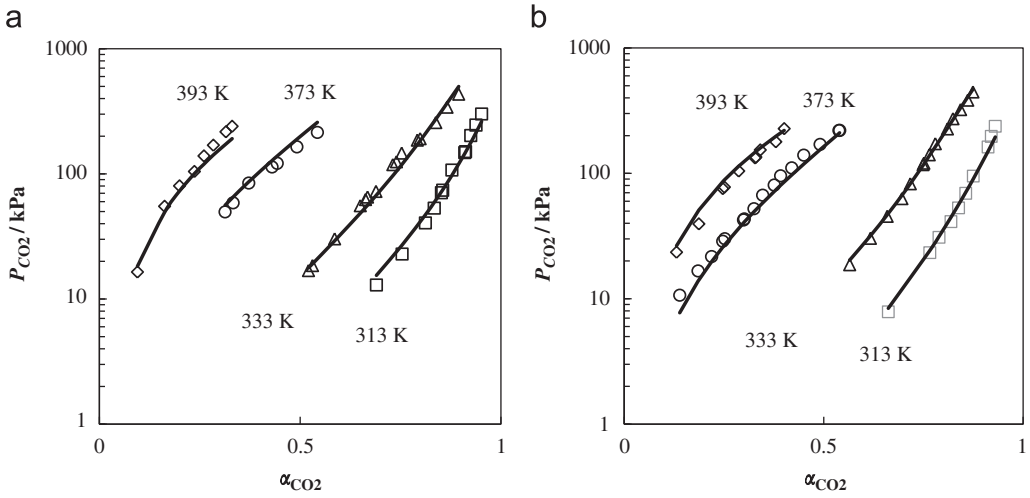


**Fig. 5.** Correlation of experimental results for AMP–PZ–$H_2O$–$CO_2$ system from this work at 313 K (□), 333 K (△), 373 K (○), and 393 K (◇); smoothed lines: model calculation. (a): 25 mass% AMP+5 mass% PZ; (b): 20 mass% AMP+10 mass% PZ.

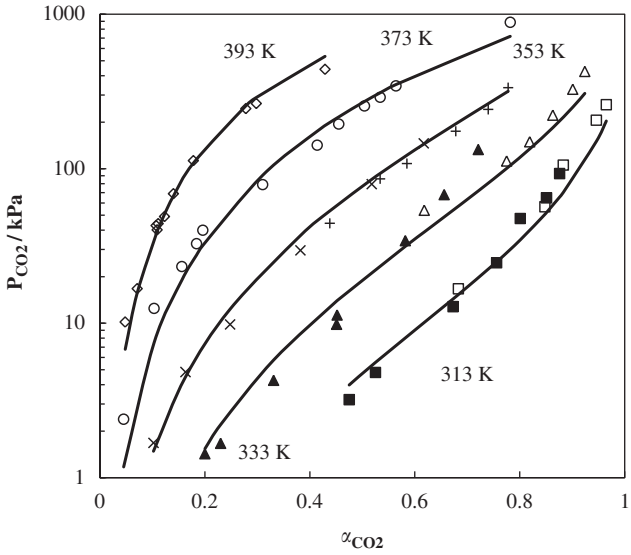


**Fig. 6.** Correlation of experimental results for AMP–$H_2O$–$CO_2$ system from this work at 313 K (□), 333 K (△), 353 K (+), 373 K (○), and 393 K (◇); Kundu et al. (2003) at 313 K (■); Li and Chang (1994) at 333 K (▲) and 353 K (×); smoothed lines: model calculation.

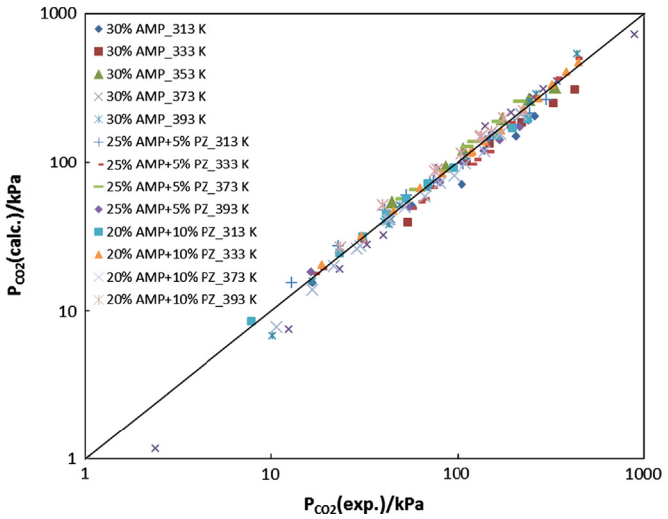


**Fig. 7.** Parity plot for the experimental data from this work and the model data for 30 mass% AMP, 25 mass% AMP+5 mass% PZ, and 20 mass% AMP+10 mass% PZ systems.

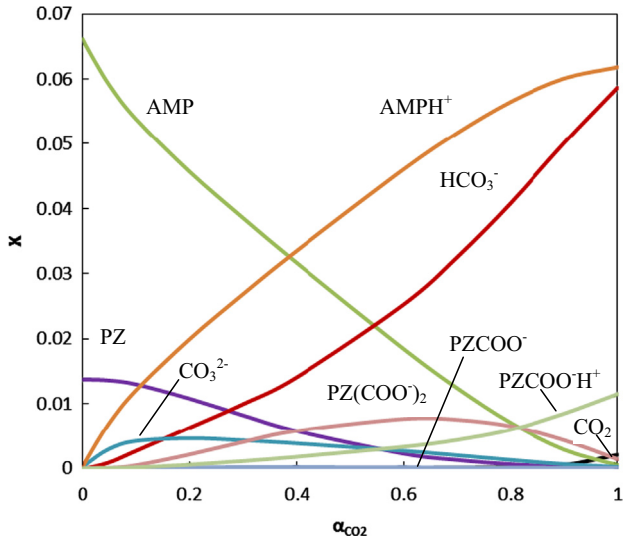


**Fig. 8.** Liquid phase speciation in aqueous 25 mass% AMP+5 mass% PZ solution at 313 K from model predictions.

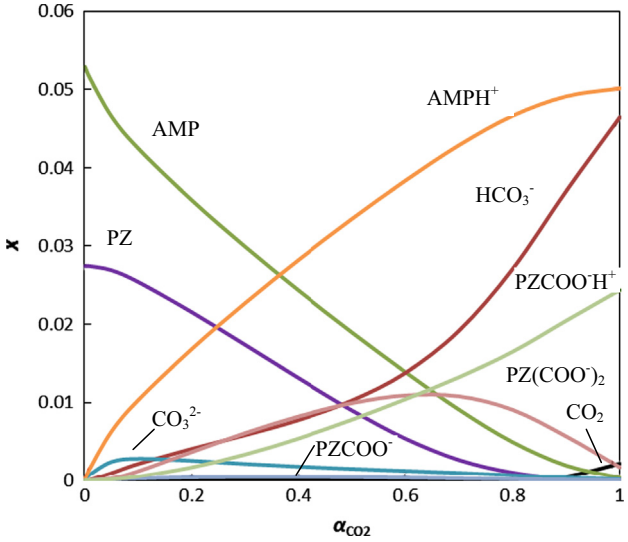


**Fig. 9.** Liquid phase speciation in aqueous 20 mass% AMP+10 mass% PZ solution at 313 K from model predictions.

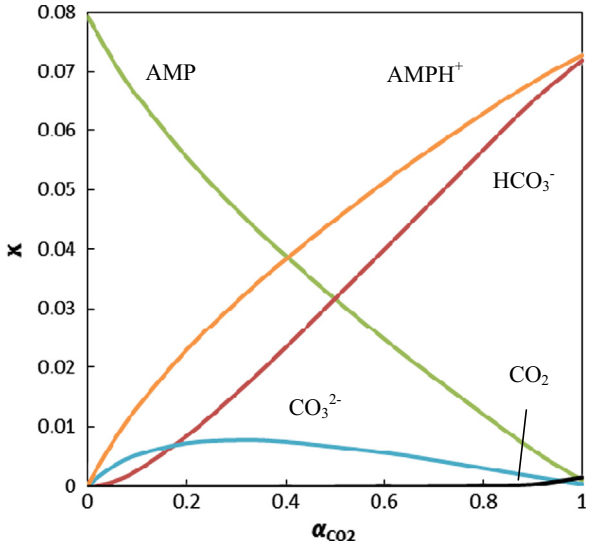


**Fig. 10.** Liquid phase speciation in aqueous 30 mass% AMP solution at 313 K from model predictions.

### 3.3. Kent–Eisenberg model for AMP–$H_2O$–$CO_2$ and AMP–PZ–$H_2O$–$CO_2$

As mentioned above, $K_7$, $K_8$ and $K_{13}$ are selected to represent the phase non-ideality and according to Eq. (15), the total number of adjustable parameters amounts to as many as 21. Some of the parameters are superfluous; as a result, a sensitivity analysis was conducted to reduce the number of adjustable parameters. The final number of adjustable parameters was reduced to the 15 listed in Table 7. This is acceptable, especially considering the complicated solution chemistry when PZ is introduced in the mixture.

The correlation results are illustrated in Figs. 5 and 6 for all the single and blended amine systems. The absolute average relative deviations, $\Delta_{AAD}$, between the model predictions of $CO_2$ partial pressure and the experimental data is 12.6%. For AMP–PZ–$H_2O$–$CO_2$, since there was no literature data at the same conditions as studied in this work, only our data were included. The $\Delta_{AAD}$ for the 25 mass% AMP+5 mass% PZ and 20 mass% AMP+10 mass% PZ are 11.1% and 8.4% respectively; for AMP–$H_2O$–$CO_2$ system, literature data from Kundu et al. (2003) at 313 K, and Li and Chang (1994) at 333 K and 353 K were also incorporated in the data regression, alongside the data from this work. The $\Delta_{AAD}$ for AMP–$H_2O$–$CO_2$ system is 15.5% for this work and 20.5% for all the literature sources.

A parity plot between the experimental data from this work and the model data is shown in Fig. 7.

Figs. 8 and 9 illustrate the speciation predictions of AMP–PZ–$H_2O$–$CO_2$ systems at 313 K from the Kent–Eisenberg model.

From the graphs, it is apparent that the concentrations of molecular amines, i.e. AMP and PZ, reduce as the solution loading increases. In the meantime, the concentrations of protonated AMP, protonated piperazine carbamate and bicarbonate rise with increasing $CO_2$ loading in the range of our model prediction. The concentrations of the second order piperazine carbamate and carbonate peak just after $\alpha=0.6$ and at $\alpha<0.1$ respectively. This is reasonable, as the increase in the $CO_2$ loading leads to rise in the solution $p$H which results in the prevalence of protonated forms of all the species. The concentration of the first order piperazine carbamate is minimal compared to other species in the solution. To summarise, the key conclusion is that PZ exists mainly in the form of $PZCOO^-H^+$ and $PZ(COO^-)_2$, whereas $PZCOO^-$ is of less importance. Besides, since the formation of AMP carbamate was neglected in our Kent–Eisenberg model, $AMPH^+$ is the only viable specie in the $CO_2$ loaded AMP solution. Finally, the most significant species derived from $CO_2$ are $HCO_3^-$, $PZ(COO^-)_2$, $PZCOO^-H^+$.

Fig. 10 shows the liquid phase speciation of 30 mass% AMP at 313 K from the Kent–Eisenberg model.

By comparing Fig. 10 with Figs. 8 and 9, it can be observed that the general trends of the major species are similar to those of mixed amine systems. One noticeable difference is that the concentration profile of $HCO_3^-$ in the mixed amines has a smaller slope at low $CO_2$ loadings followed by a steeper slope when the loading exceeds 0.6. Comparatively, the $HCO_3^-$ concentration in AMP-only solution has a quasi-linear profile. This can be explained by the presence of PZ, which preferably reacts with $CO_2$ or $HCO_3^-$ to form PZ-carbamate and reduces the concentration of $HCO_3^-$.

## 4. Conclusions

New $CO_2$ solubility data in aqueous amine blends of (AMP+PZ) were reported at temperatures between (313 and 393) K and total pressures up to 460 kPa. While maintaining the total amine mass fraction constant, the replacement of AMP with PZ reduced the $CO_2$ mole-ratio loading capacity by 8% and 12.5% for (25 mass% AMP+5 mass% PZ) and (20 mass% AMP+10 mass% PZ) respectively, compared with 30 mass% AMP. However, the mole-ratio loading capacity of the aqueous (AMP+PZ) blend still compares favourably with 30 mass% aqueous MEA: possessing over twice as much of the theoretical $CO_2$ absorption capacity as the latter. The experimental data for the AMP and (AMP+PZ) systems were also correlated with the Kent–Eisenberg model. The model can satisfactorily represent all the AMP-derived systems at temperature conditions from (313 to 393) K, giving an average absolute relative deviation of 12.6% between the experimentally determined partial pressures and those calculated from the model.

## Nomenclature

| | |
|---|---|
| $a_i$ | Adjustable parameter |
| $A_i$ | GC peak area of component $i$ |
| AMP | 2-Amino-2-methyl-1-propanol |
| $b_i$ | Adjustable parameter |
| $c_i$ | Adjustable parameter |
| $d_i$ | Adjustable parameter |
| $f_{12}$ | Response factor |
| $F$ | Objective function |
| $H_{CO2}$ | Henry's law constant for $CO_2$ in water |
| $k$ | Rate constant |
| $K_i$ | Equilibrium constant of reaction $i$ |
| $K_i'$ | Equilibrium constant deviation parameter of reaction $i$ |
| $m_i$ | Molality of species $i$ |
| $m^0$ | Standard molality, 1 mol $kg^{-1}$ |
| MEA | Monoethanolamine |
| $n_i$ | Amount of substance $i$ |
| $N$ | Number of data points |
| $P$ | Total pressure |
| $P_{CO2}$ | Partial pressure of $CO_2$ |
| $T$ | Temperature |
| $u(x)$ | Standard uncertainty of quality $x$ |

*Greek symbols*

| | |
|---|---|
| $\alpha$ | Mole-ratio loading |
| $\alpha'$ | Mass-ratio loading |
| $\Delta_{AAD}$ | Average absolute relative deviation |
| $\sigma_i^2$ | Variance of *i*th partial pressure |

## Acknowledgements

The authors appreciate the financial support from the Overseas Research Students Awards Scheme (ORSAS), the Grantham Institute at Imperial College London and Innovative Gas Separations for Carbon Capture (IGSCC) EPSRC grant EP/G062129/1.

## References

Aboudher, A., Tontiwachwuthikul, P., Chakma, A., Idem, R., 2003. Kinetics of the reactive absorption of carbon dioxide in high $CO_2$-loaded, concentrated aqueous monoethanolamine solutions. Chem. Eng. Sci. 58 (23-24), 5195–5210.
Aroonwilas, A, Tontiwachwuthikul, P., 1998. Mass transfer coefficients and correlation for $CO_2$ absorption into 2-amino-2-methyl-1-propanol (AMP) using structured packing. Ind. Eng. Chem. Res. 37, 569–575.
Bishnoi, S., Rochelle, G.T., 2000. Absorption of carbon dioxide into aqueous piperazine: reaction kinetics, mass transfer and solubility. Chem. Eng. Sci. 55, 5531–5543.
Bishnoi, S., Rochelle, G.T., 2004. Absorpion of carbon dioxide in aqueous piperazine/methyldiethanolamine. AIChE J. 48 (12), 2788–2799.
Caplow, M., 1968. Kinetics of carbamate formation and breakdown. J. Am. Chem. Soc. 90 (24), 6795–6803.
Carroll, J.J., Slupsky, J.D., Mather, A.E., 1991. The solubility of carbon dioxide in water at low pressure. J. Phys. Chem. Ref. Data 20, 1201–1209.
Chakraborty, A.K., Astarita, G., Bischoff, K.B., 1986. $CO_2$ absorption in aqueous solutions of hindered amines. Chem. Eng. Sci. 41 (4), 997–1003.
Crooks, J.E., Donnellan, J.P., 1989. Kinetics and mechanism of the reaction between carbon dioxide and amines in aqueous solution. J. Chem. Soc. Perkin Trans. II, 331–333.
Cullinane, J.T., Rochelle, G.T., 2005. Thermodynamics of aqueous potassium carbonate, piperazine, and carbon dioxide. Fluid Phase Equilibria 227 (2), 197–213.
Cullinane, J.T., Rochelle, G.T., 2006. Kinetics of carbon dioxide absorption into aqueous potassium carbonate and piperazine. Ind. Eng. Chem. Res. 45 (8), 2531–2545.
Danckwerts, P.V., McNeil, K.M., 1967. The absorption of carbon dioxide into aqueous amine solutions and the effects of catalysis. Trans. Inst. Chem. Eng. 45, T32–T49.
Dash, S.K., Samanta, A., Samanta, A.N., Bandyopadhyay, S.S., 2011. Absorption of carbon dioxide in piperazine activated concentrated aqueous 2-amino-2-methyl-1-propanol solvent. Chem. Eng. Sci. 66, 3223–3233.
Dash, S.K., Samanta, A., Samanta, A.N., Bandyopadhyay, S.S., 2011. Absorption of carbon dioxide in piperazine activated concentrated aqueous 2-amino-2-methyl-1-propanol solvent. Chem. Eng. Sci. 66, 3223–3233.
de Silva, E.F., Svendsen, H.F., 2004. Ab initio study of the reaction of carbamate formation from $CO_2$ and alkanolamines. Ind. Eng. Chem. Res. 43 (13), 3413–3418.
Edwards, T.J., Maurer, G., Newman, J., Prausnitz, J.M., 1978. Vapor–liquid equilibria in multicomponent aqueous solutions of volatile weak electrolytes. AIChE J. 24 (6), 966–976.
Ermatchkov, V., Kamps, A.P., Maurer, G., 2002. Chemical equilibrium constants for the formation of carbamates in (carbon dioxide+piperazine+water) from $^1$H NMR-spectroscopy. J. Chem. Thermodyn. 35, 1277–1289.
Haji-Sulaiman, M., Aroua, M.K., Benamor, A., 1998. Analysis of equilibrium data of $CO_2$ in aqueous solutions of diethanolamine (DEA), methyldiethanolamine (MDEA) and their mixtures using the modified Kent Eisenberg model. Chem. Eng. Res. Des. 76 (8), 961–968.
Hu, W., Chakma, A., 1990. Modelling of equilibrium solubility of $CO_2$ and $H_2S$ in aqueous amino methyl propanol (AMP) solutions. Chem. Eng. Commun. 94, 53–61.
Jou, F.Y., Mather, A.E., Otto, F.D., 1982. Solubility of $H_2S$ and $CO_2$ in aqueous methyldiethanolamine solutions. Ind. Eng. Chem. Process Des. Dev. 21, 539–544.
Kamps, A.P., Xia, J., Maurer, G., 2003. Solubility of $CO_2$ in ($H_2O$+piperazine) and in ($H_2O$+MDEA+piperazine). AIChE J. 49 (10), 2662–2670.
Kent, R.L., Eisenberg, B., 1976. Better data for amine treating. Hydro. Proc. 55 (2), 87–90.
Kundu, M., Mandal, B.P., Bandyopadhyay, S.S., 2003. Vapour–liquid equilibria of $CO_2$ in aqueous solutions of 2-amino-2-methyl-1-propanol. J. Chem. Eng. Data 48, 789–796.
Lensen, R. (2004) The promoter effect of piperazine on the removal of carbon dioxide. (Online) Available from: ⟨http://www.bsdfreaks.nl/files/hoofd6.pdf⟩ (accessed 25.03.12).
Li, M.H., Chang, B.C., 1994. Solubilities of carbon dioxide in water+monoethanolamine+2-amino-2-methyl-1-propanol. J. Chem. Eng. Data 39, 448–452.
Li, M.H., Shen, K.P., 1993. Calculation of equilibrium solubility of carbon dioxide in aqueous mixtures of monoethanolamine with methyldiethanolamine. Fluid Phase Equilibria 85, 129–140.
Littel, R.J., Versteeg, G.F., van Swaaij, P.M., 1992. Kinetics of $CO_2$ with primary and secondary amines in aqueous solutions-I. Zwitterion deprotonation kinetics for DEA and DIPA in aqueous blends of alkanolamines. Chem. Eng. Sci 47 (8), 2027–2035.
Mimura, T., Suda, T., Iwaki, I., Honda, A., Kumazawa, H., 1998. Kinetics of reaction between carbon dioxide and stericallt hindered amines for carbon dioxide recovery from power plant flue gases. Chem. Eng. Comm. 170 (1), 245–260.
Puxty, G., Rowland, R., 2011. Modelling $CO_2$ mass transfer in amine mixtures: PZ-AMP and PZ-MDEA. Environ. Sci. Technol. 45 (6), 2398–2405.
Rumpf, B., Maurer, G., 1993. An experimental and theoretical investigation on the solubility of carbon dioxide in aqueous solutions of strong electrolytes. Ber. Bunsen-Ges. Phys. Chem 97, 85–97.
Samanta, A., Bandyopadhyay, S.S., 2007. Kinetics and modelling of carbon dioxide adsorption into aqueous solutions of piperazine. Chem. Eng. Sci. 62, 7312–7319.
Samanta, A., Bandyopadhyay, S.S., 2009. Absorption of carbon dioxide into aqueous solutions of piperazine activated 2-amino-2-methyl-1-propanol. Chem. Eng. Sci. 64, 1185–1194.
Sartori, G., Savage, D.W., 1983. Sterically hindered amines for carbon dioxide removal from gases. Ind. Eng. Chem. Fundamen. 22 (2), 239–249.
Sharma, M.M., 1961. Kinetics reactions of carbonyl sulphide and carbon dioxide with amines and catalysis by Brönsted bases of the hydrolysis of COS. Trans. Faraday Soc. 61, 681–688.
Sharma, M.M., 1964. Kinetics of gas absorption. University of Cambridge, OA. (Ph.D. Dissertation).
Silkenbäumer, D., Rumpf, B., Lichtenthaler, R.N., 1998. Solubility of carbon dioxide in aqueous solutions of 2-amino-2-methyl-1-propanol and n- methyldiethanolamine and their mixtures in the temperature range from 313 to 353 K and pressure up to 2.7 MPa. Ind. Eng. Chem. Res. 37, 3133–3141.
Tong, D., Trusler, J.P.M., Maitland, G.C., Gibbins, J., Fennell, P.S., 2012. Solubility of carbon dioxide in aqueous solution of monoethanolamine or 2-amino-2methyl-1-propanol: Experimental measurements and modelling. Int. J. Greenhouse Gas Control 6, 37–47.
Vaidya, P.D., Kenig, E.Y., 2007. Absorption of $CO_2$ into aqueous blends of alkanolamines prepared from renewable resources. Chem. Eng. Sci. 62 (24), 7344–7350.
Xu, S., Wang, Y.W., Otto, F.D., Mather, A.E., 1992. Representation of equilibrium solubility properties of $CO_2$ with aqueous solutions of 2-amino-2-methyl-1-propanol. Chem. Eng. Proc. 31, 7–12.
Xu, S., Wang, Y.W., Otto, F.D., Mather, A.E., 1996. Kinetics of the reaction of carbon dioxide with 2-amino-2-methyl-1-propanol solutions. Chem. Eng. Sci. 51 (6), 841–850.
Yang, Z.Y., Soriano, A.N., Caparanga, A.R., Li, M.H., 2010. Equilibrium solubility of carbon dioxide in (2-amino-2-methyl-1-propanol+piperazine+water). J. Chem. Thermo. 42, 659–665.
Yang, Z.Y., Soriano, A.N., Caparanga, A.R., Li, M.H., 2010. Equilibrium solubility of carbon dioxide in (2-amino-2-methyl-1-propanol+piperazine+water). J. Chem. Thermo. 42, 659–665.
Yih, S.M., Shen, K.P., 1988. Kinetics of carbon dioxide reaction with sterically hindered 2-amino-2-methyl-1-propanol aqueous solutions. Ind. and Eng. Chem. Res. 27, 2237–2241.